

## BISTABLE EFFECTS IN TURBULENT FLOWS THROUGH TUBE BANKS IN TRIANGULAR ARRANGEMENTS

A. V. de Paula<sup>1</sup>, [vagtinski@mecanica.ufrgs.br](mailto:vagtinski@mecanica.ufrgs.br)

L.A.M. Endres<sup>2</sup>, [endres@ufrgs.br](mailto:endres@ufrgs.br)

S. V. Möller<sup>1</sup>, [svmoller@ufrgs.br](mailto:svmoller@ufrgs.br)

1  
Programa de Pós-Graduação em Eng. Mecânica – PROMEC  
Universidade Federal do Rio Grande do Sul – UFRGS  
Rua Sarmento Leite, 425  
90050-170 Porto Alegre, RS, Brasil

2  
Instituto de Pesquisas Hidráulicas – IPH  
Universidade Federal do Rio Grande do Sul – UFRGS  
Av. Bento Gonçalves, 9500  
91501-970 Porto Alegre, RS, Brasil

**Abstract.** *The present work describes the experimental study of the bistable phenomenon over flows through triangular tube banks, and some results for one, two and five tube rows. The bistable effect has been reported in literature for the classical arrangement of two circular cylinders placed side by side submitted to a turbulent cross flow. For this configuration, the flow who emanates through the gap between the cylinders presents a flip-flopping wake characterized by a biased flow switching at irregular intervals. This phenomenon can represent an additional source of dynamic instabilities. The aspect ratio  $p/d$  chosen was of 1.26 and 1.6, where "p" is the pitch or the distance between the centers of adjacent cylinders and "d" the diameter. The experiments are conducted in two different ways: first, the flow is investigated in an aerodynamic channel, by means of a hot wire anemometry technique. Afterwards, a flow visualization technique is applied to better understand the flow structures, in a water channel and for the interpretation of the hot wire measurements. The experimental data are analyzed by means of statistical, spectral and wavelet tools. The results show that bistability is identified in aerodynamic channel only for two rows of tubes, but with the flow visualization technique, this switching behavior is also verified for a single row of tubes. For the complete tube bank (five rows), the bistability was not verified with both techniques.*

**Keywords.** *turbulent flow; hot wires; tube banks; wavelets; flow visualization*

### 1. INTRODUCTION

In many engineering applications, circular cylinders are very common – like heat exchangers, pipelines and transmission lines. Tube banks are the most used configuration for the analysis of the phenomena that occur in several arrangements of types.

The need for more efficient heat exchangers leads the operating conditions of these equipments to become critical, due to the reduction of the aspect ratio of the tube banks (pitch-to-diameter ratio) and the increasing of the flow velocity. As a consequence of the reduction of the flow area in the narrow gaps between the tubes, which causes velocity fluctuations, and the constant change of the flow direction, static and dynamic loads will be increased (Endres *et al.*, 1995). According to Blevins (1990), the dynamic loads of the turbulent flow over small aspect ratio tube banks are characterized by broad band turbulence, without a defined shedding frequency. For large aspect ratio tube banks, the dynamic loads are basically associated with vortex shedding process.

Zdravkovich and Stonebanks (2000) comment that the leading feature of flow-induced vibration in tube banks is the randomness of dynamic responses of tubes, and even if the tubes are all of equal size, have the same dynamic characteristics, are arranged in regular equidistant rows and are subjected to an uniform steady flow, the dynamic response of tubes is non-uniform and random.

According to Païdoussis (1982), heat exchangers have been facing “spectacular failures”, which involves almost immediate failure of components, due to the flow-induced vibration.

When two circular cylinders are placed side-by-side and submitted to a turbulent cross-flow, an interesting phenomenon occurs: the flow that emanates through the gap between the cylinders is biased towards the rear surface of one of the cylinders, and has a narrow wake. This can be called as a flow mode. When a floppy and random behavior of the gap flow changes intermittently the flow mode, from one cylinder to other at irregular time intervals, in literature, this is the so called *bistability* phenomenon.

Triangular geometry was chosen in this work due to the fact that several engineering applications have been using it, and also because bistability has been found more recently in tube banks with square arrangement (Olinto *et al.*, 2006). Besides, as flow induced vibration and fluid-structure interaction are very dependent on the configuration or arrangement of the cylinders (side-by-side or tandem), which can be an additional excitation mechanism of the tubes, a need of new information about this phenomenon is necessary.

Flow visualization techniques can be applied to the better comprehension of the phenomena studied in laboratory conditions. Alam *et al.* (2005) present a flow visualization study to the determination of flow configurations and fluid forces acting on two staggered circular cylinders of equal diameter in cross-flow. Olinto (2005) determined through

experiments the presence of a biased and bistable flow mode of two cylinders placed in a side-by-side arrangement, and also presented flow visualization results of this configuration using a water channel. Ziada (2006) presents a flow visualization study about vortex shedding, acoustic resonance and turbulence excitations in tube bundles in triangular arrangements of cylinders at various Reynolds numbers and pitch-to-diameter ratios.

## 2. THE BISTABLE EFFECT

According to Sumner *et al.* (1999) the cross steady flow trough circular cylinder with same diameter ( $d$ ) placed side-by-side can present a wake with different modes, depending on distances between its centers, called pitch ( $p$ ). Different flow behaviors can be found for different pitch-to-diameter ratios  $p/d$ . For the case when  $1.2 < p/d < 2.0$  (also called intermediate pitch ratios), the flow is characterized by a wide near-wake behind one of the cylinders and a narrow near-wake behind the other, as shown schematically in Fig. 1a and Fig. 1b. This phenomenon generates two dominants vortex-shedding frequencies, each one associated with a wake: the wide wake is associated with a lower frequency and the narrow wake with a higher one.

Bistable phenomenon is characterized by a switching of this gap flow, which is biased toward the cylinder, from one side to other at irregular time intervals. For the two side-by-side cylinders case, a link between the wakes patterns, show in Figs. 1a and 1b, and a velocity measurement technique (as the hot wire anemometry technique) can be established through the Fig. 1c. This figure shows the velocity signals measured downstream the cylinders, along the tangent to their external generatrices, where one switching mode can be observed (modes A and B). Previous studies show that this pattern is independent of Reynolds number, and it is not associated to cylinders misalignment or external influences, what suggest an intrinsically flow feature.

According to Kim and Durbim (1988) the transition between the asymmetric states is completely random and it is not associated with a natural frequency. Through a dimensional analysis, they concluded that the mean time between the transitions is on order  $10^3$  times longer than vortex shedding period, and the mean time intervals between the switches decreases with the increasing of Reynolds number. The authors conclude that there is no correlation between the bistable feature and the vortex shedding, due to the fact that Strouhal numbers are relatively independent from the Reynolds numbers (Žukauskas, 1972).

Williamson (1985), studying the vortex wakes produced by the flow behind a pair of bluff bodies placed side-by-side in a stream, found a steady mean flow for  $Re=200$ , using flow visualization techniques (both smoke in a wind tunnel and dye in a water channel).

Indrusiak *et al.* (2005), studying the velocity and pressure fluctuations of transient turbulent cross-flow in a tube bank with square arrangement and a pitch-to-diameter ratio of 1.26, determined experimentally the presence of a biased and bistable flow mode inside a tube bank, behind the third row of tubes. Transient and steady state flows were studied, by means of accelerating and decelerating the centrifugal blower of the aerodynamic channel. Wavelet and wavelet packet multiresolution analysis, together with continuous wavelet transform were applied, and the results show that the flow through tube banks has an unsteady three-dimensional nature.

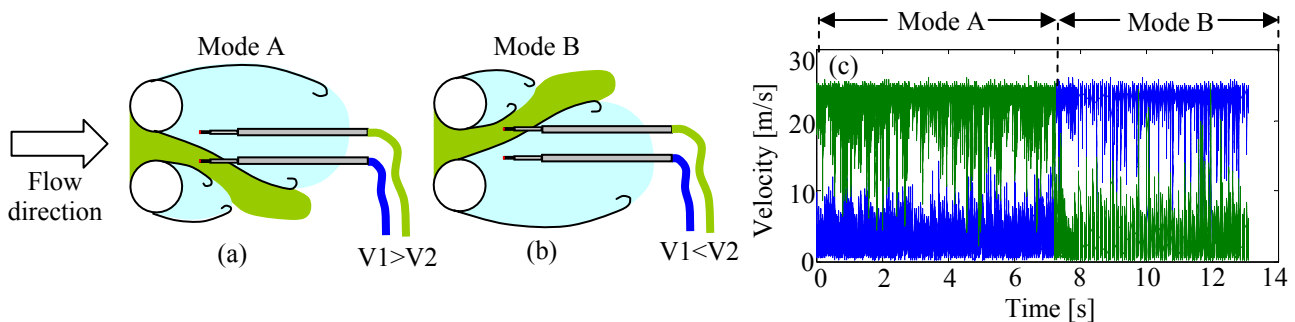


Figure 1. Bistability scheme for (a) mode A and (b) mode B, and the respective characteristic signals (c).

## 3. OBJECTIVES

The purpose this experimental work is to study the presence of bistable flows in tube banks with triangular arrangements, determine their characteristics and conditions of formation.

## 4. THE EXPERIMENTAL TECHNIQUE

Two experimental techniques were used in this work. Hot-wire anemometry in an aerodynamic channel was applied to measure velocity and velocity fluctuations in several tube banks. The analysis was seconded by flow visualizations performed in a water channel. The Reynolds numbers for all the experiments were calculated with the percolation velocity, the diameter of the cylinders and the kinetic viscosity of the fluid. The percolation velocity takes in consideration the porous area of the test section, in a top view, and depends on the reference velocity and the relation of

the areas occupied by the cylinders and the whole tube bank area. Physically, it is the mean velocity of the tube bank in a top view. Endres and Möller (2001) present a more complete study of the use of this parameter in tube-bank flow analysis.

#### 4.1. Aerodynamic channel

The velocity of the flow and its fluctuations are measured by means of the DANTEC *StreamLine* constant hot-wire anemometry system, with aid of two hot wire probes (type DANTEC 55P11), with single wires perpendicular to the main flow. The wires of both probes were maintained in horizontal position, and the measurements were performed aligning the probes along the tangent to the external generatrices of two adjacent tubes. The aerodynamic channel used in the experiments is made of acrylic, with a rectangular test section of 0.146 m height, width of 0.193 m and 1.02 m of length (Fig. 2a). The air is impelled by a centrifugal blower of 0.64 kW, and passes through two honeycombs and two screens, which reduce the turbulence intensity to about 1% in the test section. Upstream the test section, placed in one of the side walls, there is a Pitot tube, which measures the reference velocity of the non-perturbed flow. The data acquisition is performed by a 16-bit board (NATIONAL INSTRUMENTS 9215-A) with USB interface, which converts the analogical signal to digital series. The tubes are rigidly attached to the top wall of test section, and the probe support is fixed in both side walls of the channel (Fig. 2b). The mean error of the flow velocity determination with a hot wire was about 3%.

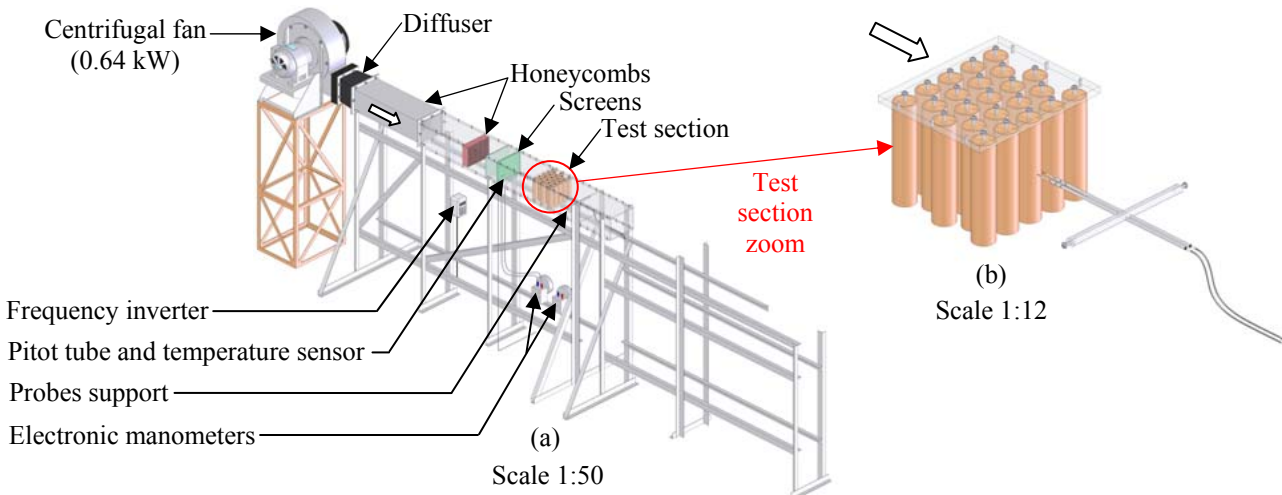


Figure 2. Schematic view of (a) the aerodynamic channel and (b) test section.

#### 4.2. Water channel

Flow visualizations were performed in the closed circuit water channel of the Hydraulic Research Institute of the Federal University of Rio Grande do Sul. The water channel has a settling chamber with a honeycomb which acts as a flow straightener, a nozzle, a 30 m long open channel (10 m upstream, 20 m downstream the test section) with 0.5×0.6 m rectangular cross section, a vertical gage to control the water level, and a discharge tank with the return pipe to close the circuit. The flow rate is read by an electromagnetic flowmeter and can vary from 0.0006 m<sup>3</sup>/s to 0.22 m<sup>3</sup>/s, resulting in velocities from 3×10<sup>-3</sup> m/s to 1.1 m/s\*. The maximum flow depth is 0.5 m which is controlled through the flow rate, by a set of valves in the feeding pipeline, and by the vertical gage placed in the discharge.

The experiments are conducted inside a visualization section (Fig. 3a), which consists on a tube bank with  $p/d = 1.26$  and  $p/d = 1.6$ , inside a channel placed in the visualization section of the water channel. The tube banks had 1, 2, 3, 4 and 5 rows. The upper plate was placed 0.08 m below the water level to reduce the effect of gravitational waves. The water level is maintained at 0.38 m in the test section for all experiments. The cylinders are rigidly attached to the base plate, and are built with commercial PVC tubes, with diameter of 0.06 m, covered by a thin white PVC film (Fig. 3c). Inside each cylinder, there are six hoses, distributed in the following mode: 2 hoses at 0.06 m below the ceiling plate of acrylic, 2 hoses at the middle plane of the visualization section (at 0.15 m from the base or the ceiling plate) and 2 hoses at 0.06 m above the base plate of acrylic. Each one of these pairs of hoses exits with an inclination of 10° with the horizontal plane (one hose in relation to another). So, visualizations can be performed in these three planes, with different ink colors. In each row, one of the cylinders is provided with an inclined movable mirror to observe the behavior of the ink flow of the neighboring cylinder, in the path indicated by the Fig. 3b. The mirror can be moved up and down by a steel cable and a spring (Fig. 3d). A typical view through the mirror is shown in Fig. 3e.

\* These values are obtained with a water level of 0.4 m

An ink distribution system was mounted to provide an adequate ink injection in the cylinders. It consists of 15 tanks, with red, green and blue ink (respectively the inferior plane, middle plane and top plane of visualization), each one with a volume about  $0.002 \text{ m}^3$ , connected by PVC hoses to valves that control the ink flow through a complex ink distribution system under the base plate to the tubes and then to injection taps drilled on the tube walls. The base plate is covered by a thin white PVC film with purpose of enhancing the contrast of the ink traces and for lightning distribution. A Sony digital camera, placed above the bank, was used for taking picture shots (4.1Mp) or digital movies (VGA -  $640 \times 480$  pixels, 30 frames per second). The results of the flow visualizations are presented through static pictures, obtained from the movies, where the flow direction is from the left to the right.

Velocities profiles inside the visualization section were measured with a hot film probe (type DANTEC 55R42), in a vertical plane at  $0.05 \text{ m}$  upstream the outlet, where the flow in the water channel presents a small velocity asymmetry.

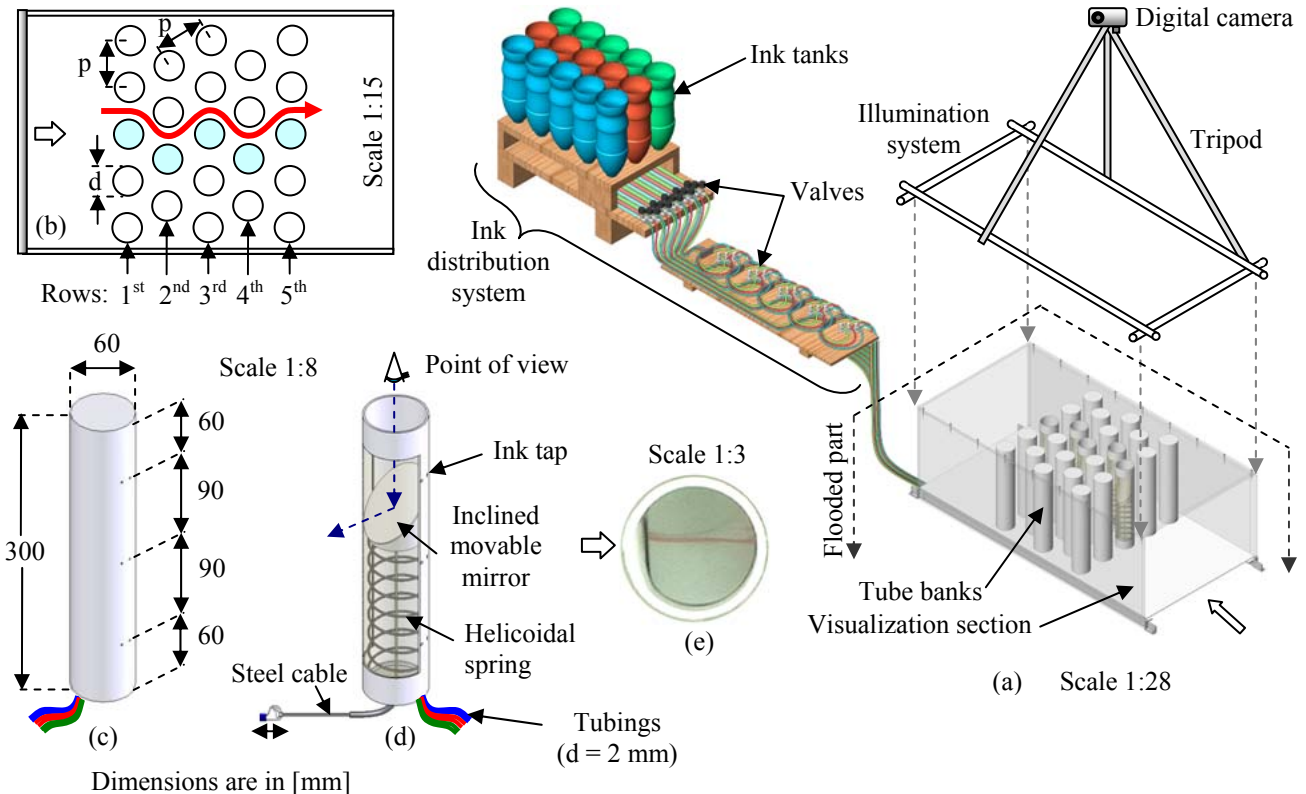


Figure 3. (a) Schematic illustration of the ink distribution system and the tube banks inside the visualization section. (b) Detail of the tube banks (top view) and the special tubes with inclined movable mirrors. (c) Schematic illustration of the tubes: (a) solid tubes and (b) tubes with inclined movable mirrors. (d) Detail of flow through the mirror view. (e) Detail of flow through the mirror view.

## 5. MATHEMATICAL TOOLS

The analysis of a time series can be performed in time domain, frequency domain and joint time-frequency domain.

The time domain analysis consists on the determination the four moments of the probability density function: mean (average), standard deviation, skewness and kurtosis. A frequency domain analysis can be done through the power spectral density function (PSD). According to Bendat and Piersol (1971), the PSD function gives the energy distribution of the signal in frequency domain. In this case, the stationary hypothesis of a time signal must be accomplished. The ensemble time-frequency domain analysis was made trough wavelet transform. Basically, a wavelet analysis is applied to time varying signals, where the stationary hypothesis cannot be maintained. Thus, discrete and continuous wavelet transforms can be used:

- *Discrete Wavelet Transform* (DWT): used to make a multilevel decomposition of a time signal in several bandwidth values, accordingly with the selected decomposition level.
- *Continuous Wavelet Transform* (DWT): used to analyze the energy content of a signal through the so called spectrogram.

In this work, Daubechies “db20” functions were used as bases of both discrete and continuous wavelet transforms. Indrusiak (2004) presents a more complete review of discrete and continuous wavelet transforms, applied to accelerating and decelerating turbulent flows. All mathematical analysis was made with Matlab ® software and its specific toolboxes for statistical, spectral and wavelet analysis.



## 6. RESULTS

### 6.1. One row of cylinders

The study of the flow through a row of five circular cylinders was conducted in the aerodynamic channel by placing two hot wire probes aligned with the tangent to the external generatrices of two adjacent tubes (Fig. 4a), in each one of the gaps. This figure refers to the complete tube bank. For the experiments performed with one row of cylinders, the other four rows were taken off, and so on.

The Reynolds number for this experiment is  $Re = 4.43 \times 10^4$ , with a percolation velocity ( $U_{per}$ ) of 26.8 m/s. The signals obtained from a 3 kHz acquisition frequency, in the gap 2, at a distance of 0.01 m downstream the cylinders are shown in Figs. 5a and 5b, for the aspect ratios of  $p/d = 1.26$  and 1.6, respectively. Their discrete wavelet reconstructions of level 9 (which provides frequencies from 0 to 2.93 Hz) are shown in Figs. 5c and 5d, where no bistable effect can be identified. Figures 5e and 5f show the power spectral density functions calculated from the velocities signals. For aspect ratio  $p/d = 1.26$  (Fig. 5e), two peaks are visible in the power spectrum: the first is at 60 Hz, which corresponds to a Strouhal number ( $S$ ) of 0.04 and is not so strikingly, and the second is at 259 Hz, which corresponds to  $S=0.17$ . The Strouhal numbers are calculated with the gap velocity (37.5 m/s). For aspect ratio  $p/d = 1.6$  (Fig. 5f), there are two sharp peaks in the power spectrum: one is at 220 Hz, which corresponds to  $S=0.15$ , and other is at 500 Hz ( $S=0.33$ ).

Table 1 shows the mean and RMS values obtained from the velocity signals for all the four gaps and two  $p/d$  ratios. Tracing a centerline exactly in the middle distance between two adjacent cylinders, aligned with the flow direction (Fig. 4b), it is possible to perform a qualitative analysis of the flow pattern by comparing the mean values of the velocity signals, for a given gap. From this figure, for example, if  $\bar{V}_2$  is greater than  $\bar{V}_1$ , it means that the gap flow is biased towards the upper cylinder. So, probe 2 is measuring the high velocity of the gap flow, and probe 1 is measuring the flow inside the wide near-wake.

Figures 6a and 6b show the results of the flow visualization for one row of cylinders, with  $Re = 7.5 \times 10^3$ , and  $p/d = 1.26$  and  $p/d = 1.6$ , respectively, where it is possible to see that a wide near-wake is formed downstream the central cylinder. This was the first stable flow pattern observed in the flow visualizations. The schematic flow patterns for this case, produced by the technique above mentioned are also shown in this figure, where the results are in good agreement with flow visualizations. The details of the lateral of the tubes are shown in Fig. 6c, where no important vertical component is visible. From the details of the inclined mirror (plan view: (top - Fig. 6d), (middle - Fig. 6e) and (bottom - Fig. 6f)) is possible to see that the flow remains predominantly two-dimensional.

However, other patterns were also found in the flow visualizations. Figure 7a shows the second flow pattern found for  $Re = 7.5 \times 10^3$  and  $p/d = 1.26$ , where a near wide-wake is present behind the second cylinder, from up to bottom. The third identified flow pattern shown to be bistable, where the second cylinder, from bottom to up, presents a narrow near-wake (mode A - Fig. 7b). After a certain time interval, this cylinder presents a wide near-wake (Mode B - Fig. 7c). For the Reynolds number of  $1.5 \times 10^4$  and for the visualization planes not mentioned, the results are similar.

One of the possible causes of the discrepancy of these results can be attributed to the difference between mean turbulence intensity values ( $TI$ ) of the experimental techniques\* (hot wire anemometry in aerodynamic channel:  $TI \approx 1\%$ , and flow visualization in water channel:  $TI \approx 5\%$ ).

Summarizing, in the most part of the cases, the wake pattern observed was stable. It means that the flow who emanates from the gaps between the cylinders form coalescent jets, with the formation of a wide near-wake behind one of the cylinders, and a narrow near-wake behind their neighbors. For consecutive experiments, this pattern can be changed, and the wide near-wake, which was behind a specific cylinder, can be now behind another one. However, in some cases the wake pattern observed was bistable, with the formation of a changing flow direction at irregular intervals. All this behavior is in accordance with the results of Zdravkovich and Stonebanks (1988) and Zdravkovich (1997), which was called by the authors as "metastable".

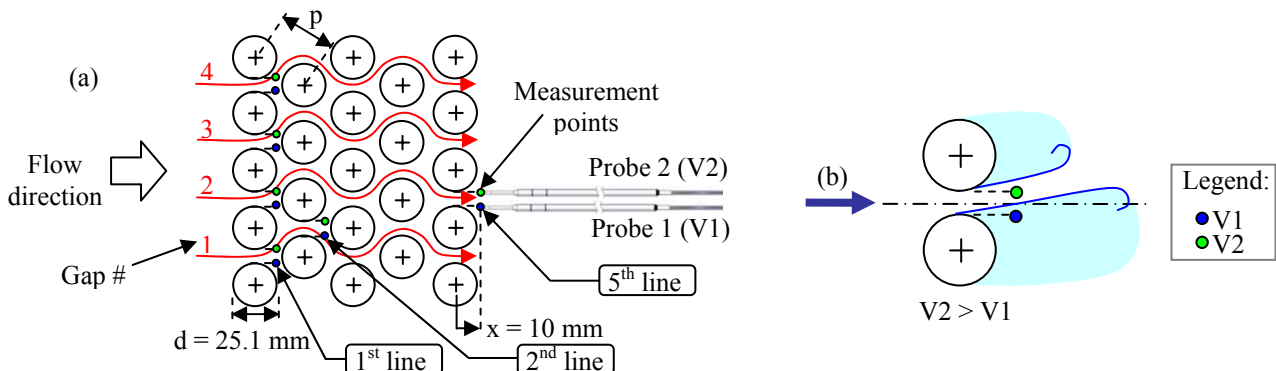


Figure 4. (a) Schematic view of all the experiment and probes positions. (b) Schematic view of the gap flow.

\* These values are referent to the center of the channels.

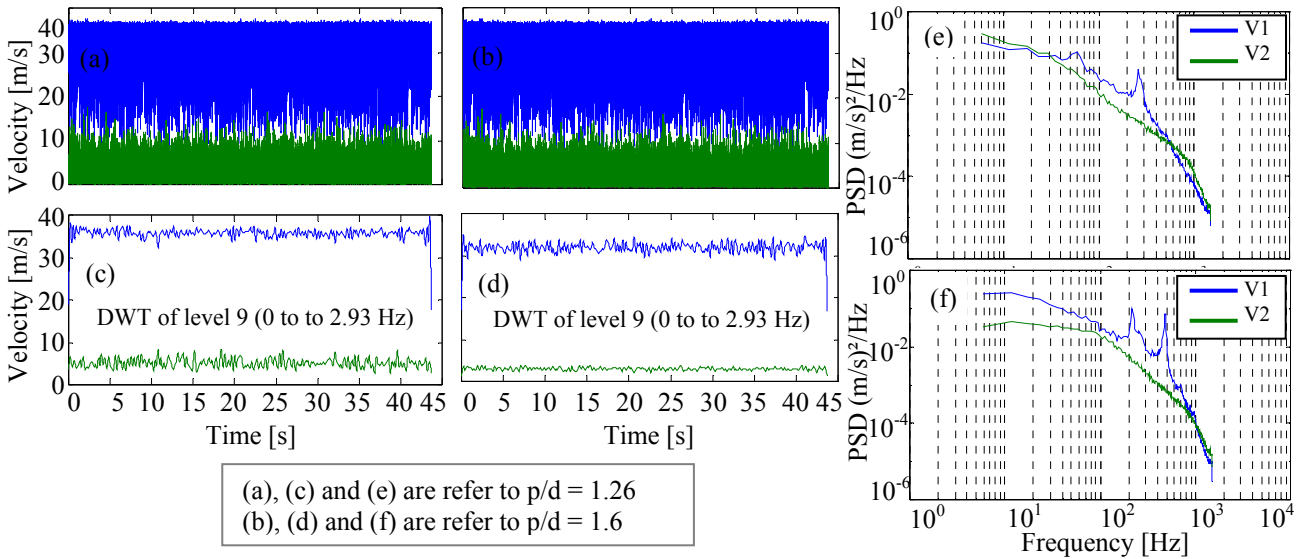


Figure 5. (a) and (b) are the measured velocity signals in the gap 2. (c) and (d) are the reconstructed signals using DWT. (e) and (f) are the power spectral density functions calculated from the signals.

Table 1. Mean and RMS values of the measurement velocities series in the gaps of one row of cylinders.

Gap	$p/d = 1.26$				$p/d = 1.6$			
	Mean [m/s]		RMS [m/s]		Mean [m/s]		RMS [m/s]	
	V1	V2	V1	V2	V1	V2	V1	V2
1	7.82	8.58	8.96	9.58	3.46	28.28	4.05	28.43
2	30.17	3.65	30.26	4.31	31.97	2.92	32.24	3.59
3	3.88	27.95	4.41	28.04	3.22	24.87	3.88	25.56
4	9.61	6.94	10.72	8.31	3.22	24.87	3.88	25.56

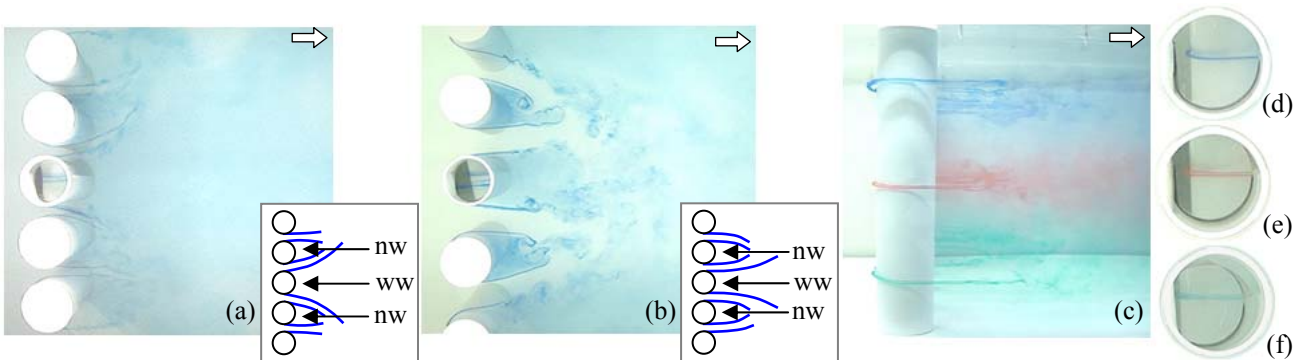


Figure 6. Flow visualizations of a row of cylinders at  $Re = 7.5 \times 10^3$  with their respective schematic flow patterns in the top plan view: (a)  $p/d = 1.26$  and (b)  $p/d = 1.6$ . (c) Details of the lateral of the tubes. Details of the inclined mirror: (d) top, (e) middle and (f) inferior plan view. Legend: "nw" means wide near-wake and "ww" means narrow near-wake.

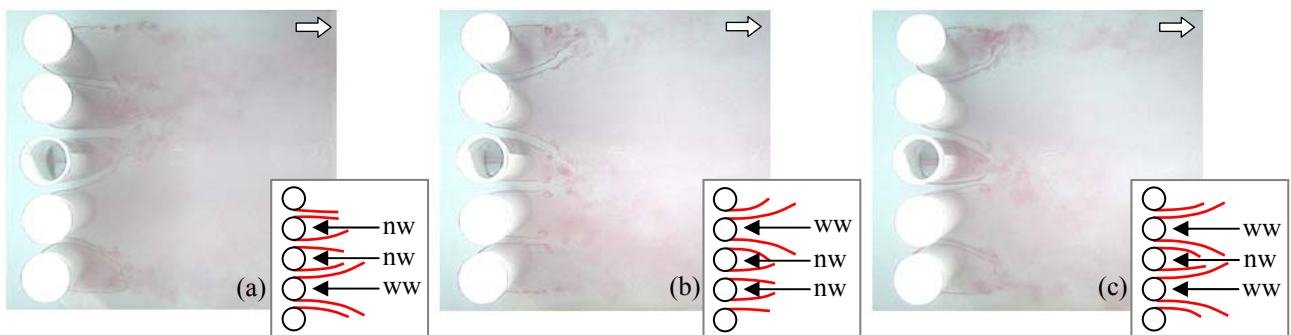


Figure 7. Flow visualizations of a row of cylinders at  $Re = 7.5 \times 10^3$  with their respective schematic flow patterns. Middle visualization plan and  $p/d = 1.26$ . (a) Second flow pattern identified. The third flow pattern shown to be bistable: (b) mode A and (c) mode B. Legend: "ww" means wide near-wake and "nw" means narrow near-wake.

## 6.2. Two rows of cylinders

The study of the flow through two rows of circular cylinders in triangular arrangement was conducted in a similar way of one row of cylinders. The positions of the hot wire probes for this experiment are also shown by Fig. 4a, which the results concern to gap 1. For  $p/d = 1.26$ , the Reynolds number was  $Re = 3.79 \times 10^4$  ( $U_{per} = 22.9$  m/s), and for  $p/d = 1.6$ ,  $Re = 3.45 \times 10^4$  ( $U_{per} = 20.9$  m/s). The experiments were performed by turning on and off the blower of the aerodynamic channel, to measure the transient flow: from rest to the steady state and vice-versa.

For  $p/d = 1.26$  the signals obtained from a 1 kHz acquisition frequency, at a distance of 0.01 m downstream the cylinders are shown in Figs. 8a and 8b for probes 1 and 2, respectively. These signals, referred to the starting flow, show three changes of the flow mode: two fast changes ( $t=53.2$  to 54.9 seconds, and from  $t=63.3$  to 64.4 seconds) that last 1.7 and 1.1 seconds, respectively, and one that starts at  $t=80$  seconds and remains until the finish of the acquisition. Their discrete wavelet reconstructions of level 9 (which provides frequencies from 0 to 0.48 Hz) are shown in Fig. 8c, where is observed that the first two fast changing occur in a symmetric way, by maintaining the mean flow velocity. The third and last changing seems to happen in a non-symmetric way, due to a different mean flow velocity.

Figures 8d and 8e show the signals obtained for  $p/d = 1.6$  (with a 3 kHz acquisition frequency) for probes 1 and 2, respectively. From 0 to 12 seconds the flow is accelerated from the rest to the steady state. After this time interval and until  $t = 36$  seconds (steady state flow), no bistable effect was detected. The time interval between  $36 < t < 62$  seconds concerns to flow deceleration followed by a new acceleration, to simulate the execution of consecutive experiments. After  $t = 62$  seconds (steady state flow), again, no significant changes of the mean velocity values are observed. However, the mean velocity level of both steady state flow intervals are modified, which means that the gap flow has no preferred direction. This behavior is clearly observed through the discrete wavelet reconstructions of level 9 (frequencies from 0 to 1.46 Hz), shown in Fig. 8f.

By separating two intervals of these signals, it is possible to statistically analyze the flow modes. For  $p/d = 1.26$ , the chosen interval was: Mode A, from  $t=15$  to  $t=47.8$  seconds, and Mode B, from  $t=92.2$  to  $t=125$  seconds, each mode with 32768 data points. For  $p/d = 1.6$ , Mode A corresponds from  $t=13$  to  $t=34.8$  seconds, and Mode B, from  $t=65$  to  $t=86.6$  seconds, each mode with 65536 data points. Table 2 shows that the statistical characteristics of the velocity series for both aspect ratios and flow modes changes. It is observed that the statistical characteristics of each flow mode are carried by the switching between the velocities of the both probes. This behavior is associated to the switching in the gap flow direction. Figure 9 shows the power spectral density functions referred to each one of these intervals. For  $p/d = 1.26$  (Figs. 9a and 9b) there is a changing in the energy content between the modes, but no sharp peak in the spectrum is present. For  $p/d = 1.6$  (Figs. 9c and 9d) the spectrums present a sharp peak in 710 Hz, which corresponds to a Strouhal number of 0.665, referent to the gap velocity (26.8 m/s).

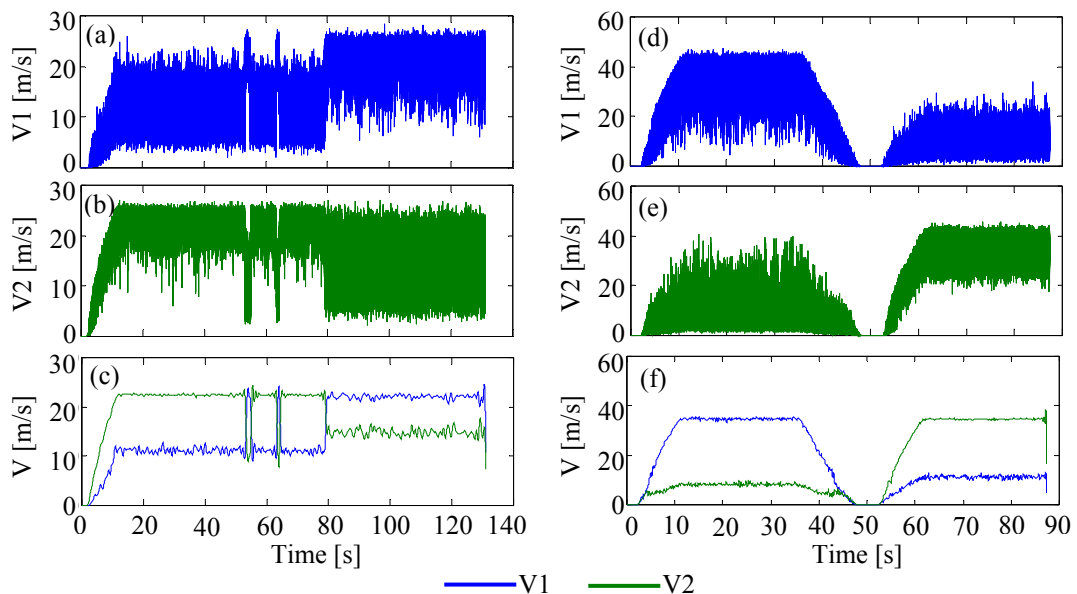


Figure 8. (a) and (b) measured velocity signals for  $p/d = 1.26$ . (d) and (e) measured velocity signals for  $p/d = 1.6$ . (c) and (f) reconstructed signals using DWP. Results for gap 1.

Figure 10 shows the results of the flow visualizations for two rows of cylinders with the injection of potassium permanganate directly in the free stream at  $Re = 7.5 \times 10^3$ , with  $p/d = 1.6$  in the middle visualization plan with the respective schematic flow patterns. For mode A (Fig. 10a) there is a wide near-wake behind the second cylinder, from right to left. After 70 seconds (mode B - Fig. 10b) this cylinders presents a narrow near-wake. The details of the inclined mirrors in the three visualization plans with ink dye technique are shown in Figs. 10c, 10d and 10e, where the

flow in the first row of cylinders remains predominantly two-dimensional, and after the second row it turns three-dimensional, with some vertical transversal fluctuations. Other three flow patterns were also found for this arrangement.

Table 2. Statistical characteristics from the velocity series after two rows of cylinders, in gap 1.

	p/d = 1.26				p/d = 1.6			
	Mode A		Mode B		Mode A		Mode B	
	V1	V2	V1	V2	V1	V2	V1	V2
Mean velocity [m/s]	11.16	22.45	22.08	14.86	34.70	8.22	11.26	34.58
Standard deviation [m/s]	3.33	1.61	2.39	4.46	5.18	4.13	3.57	3.72
Skewness	0.42	-1.23	-1.48	-0.08	-0.52	1.65	0.20	0.28
Kurtosis	2.91	7.48	6.57	2.32	3.66	7.81	3.20	2.94

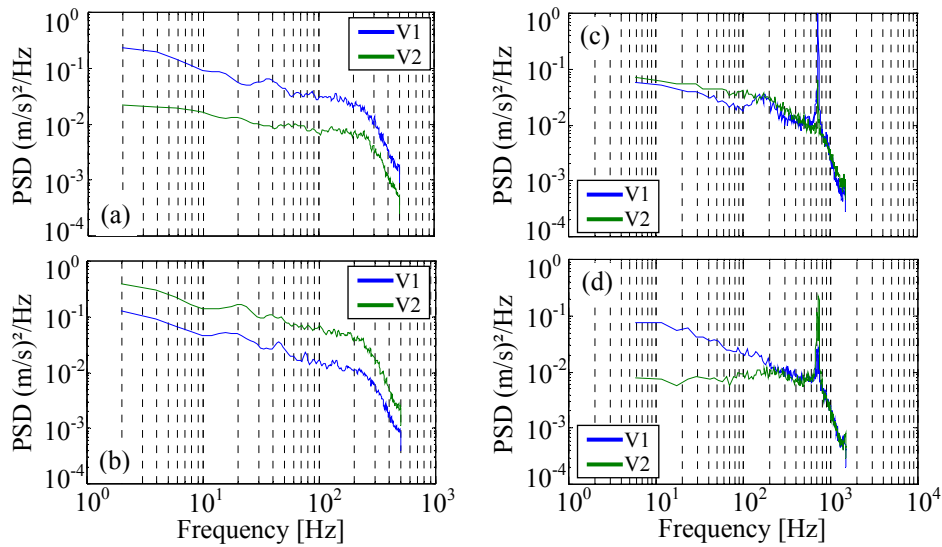


Figure 9. Power spectral density functions calculated from the velocity signals for the gap 1. (a) and (b) refer to p/d = 1.26, modes A and B, respectively. (c) and (d) refer to p/d = 1.6, modes A and B, respectively.

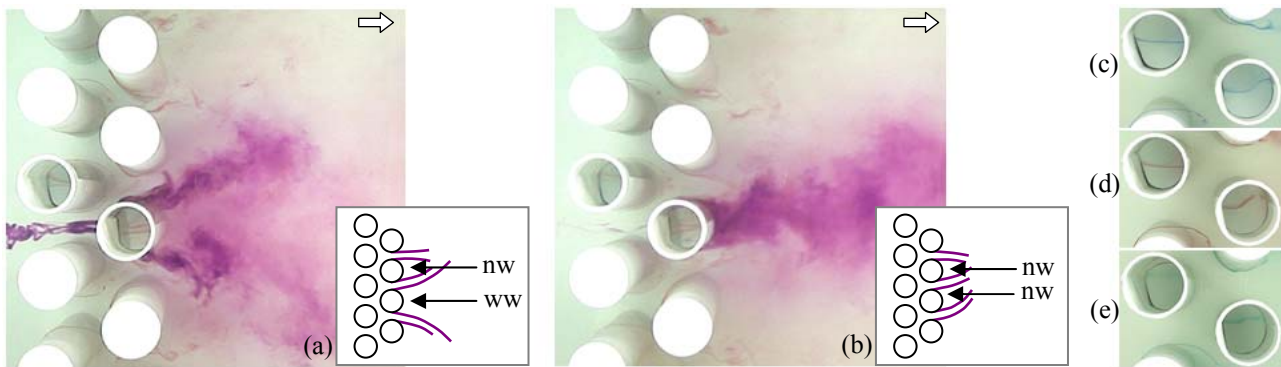


Figure 10. Flow visualizations of two rows of cylinders at  $Re = 7.5 \times 10^3$ , with  $p/d = 1.6$  in the middle visualization plan and the respective schematic flow patterns: (a) mode A and (b) mode B. Details of the inclined mirrors: (c) top, (d) middle and (e) inferior plan view. Legend: “ww” means wide near-wake and “nw” means narrow near-wake.

### 6.3. Three, four and five rows of cylinders

The leading feature of turbulent flow through tube banks of triangular arrangement after three, four and five rows of cylinders seems to be similar, for both aspect ratios studied. For these cases, the flow who emanates from the gaps between the cylinders presents a fast swapping, from one side to another (flip-flop). Furthermore, the results for the fifth row of cylinders (complete tube bank) will be presented (Fig. 4a), referent to  $p/d = 1.6$ . From the obtained velocity signals (Figs. 11a and 11b), no special features can be observed, but after a reconstruction by discrete wavelet of level 10 (frequencies from 0 to 0.488 Hz) this flip-flop behavior appears (Fig. 11c). For  $p/d = 1.26$ , the Reynolds number was maintained in the range of  $Re = 3.38 \times 10^4$  to  $3.63 \times 10^4$  ( $U_{per} = 20.2$  m/s to 22.0 m/s), and for  $p/d = 1.6$ ,  $Re = 3.01 \times 10^4$  to  $3.25 \times 10^4$  ( $U_{per} = 18.3$  m/s to 19.7 m/s). From the discrete wavelet reconstructions and from the cross-correlation



functions (Fig. 12a) is possible to observe that the velocity signals are  $180^\circ$  out of phase. The power spectral density functions (Fig. 12b) present no peak and the energy content of the both signals are very similar. The continuous wavelet transform (spectrogram) of the signals are presented in Figs. 12c and 12d, where a large energy spreading is observed for many frequencies. The results of the flow visualizations for  $Re = 7.5 \times 10^3$  and  $p/d = 1.6$  are shown in Fig. 13. Figures 13a to 13e show the results obtained for the ink injection, from the first row of cylinders until the fifth, where a transverse vertical component is present, after the second row of cylinders. This feature increases after the third, fourth and fifth rows, where the three-dimensional effects are more evident. Figures 13f to 13j show the results with the injection of potassium permanganate directly in the free stream, where a highly disordered flow is observed. This flip-flop flow behavior seems to be strongly influenced by the presence of the tubes of the next row. Due to this effect, the flopped flow will be directed parallelly to the tubes axes (up or downwards), so that the flow through tube banks will give a strong three-dimensional characteristic.

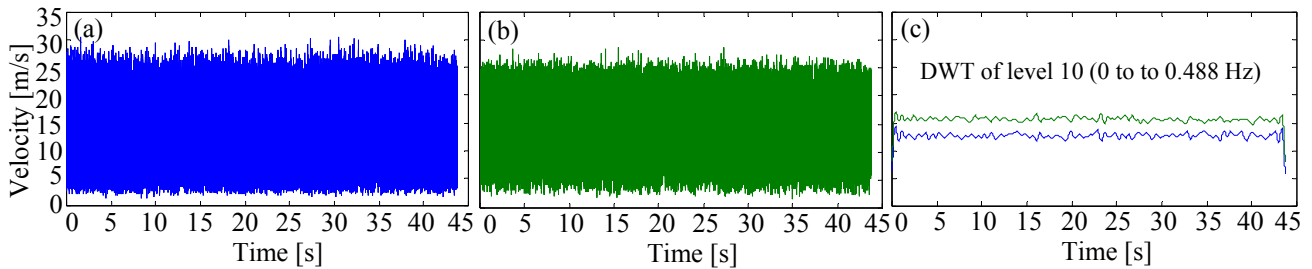


Figure 11. Results for  $p/d = 1.6$ . (a), (b) Velocity signals obtained after five rows of tubes. (c) Reconstructed signals using DWT.

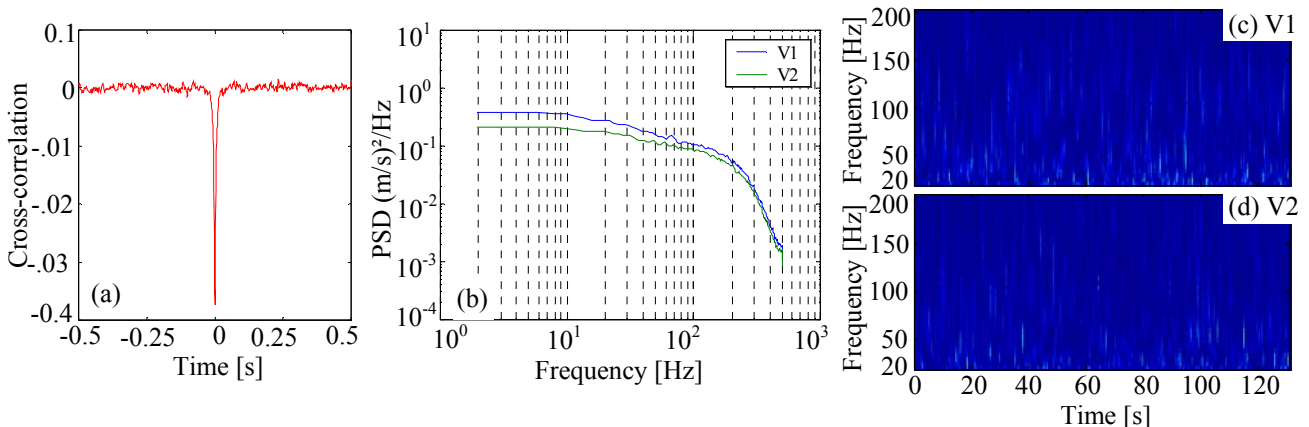


Figure 12. Results for  $p/d = 1.6$ . (a) Cross-correlation function of the velocity signals. (b) Power spectral density functions of the velocity signals. (c), (d) Continuous wavelet transform (spectrogram).

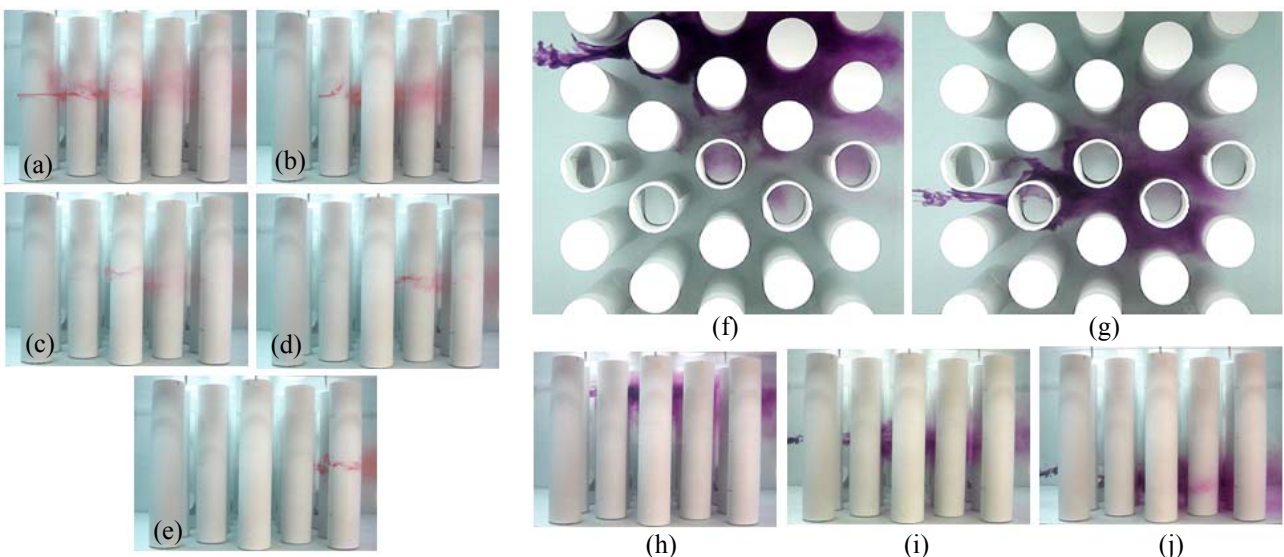


Figure 13. Flow visualizations of five lines of cylinders at  $Re = 7.5 \times 10^3$ , with  $p/d = 1.6$ . From (a) to (e) are the results obtained for the ink injection technique, from the first line of cylinders until the fifth. From (f) to (j) are the results with the injection of potassium permanganate directly in the free stream.

## 7. CONCLUSIONS

This paper presents the experimental study of bistable flow in tube banks of triangular arrangement. This phenomenon can be an addition excitation mechanism of the tubes. The pitch-to-diameter ratios were  $p/d=1.26$  and  $p/d=1.6$ . Hot wire anemometry technique was used to measure the velocity fluctuations of the air flow in the aerodynamic channel, and the dye injection technique was used in the flow visualizations performed in the water channel.

For one row of cylinders, the tests performed with aerodynamic channel present a stable wake pattern. However, in water channel visualizations, for consecutive experiments, this pattern can be changed, and the wide near-wake, which was behind a specific cylinder, can be now behind another one. Only in some cases the wake pattern observed was bistable, with the formation of a changing flow direction at irregular intervals. This behavior is called in literature as “metastable”, and the results have good agreement with the results of Zdravkovich and Stonebanks (1988).

For two rows of tubes the occurrence of bistability is clearly identified for  $p/d = 1.26$  aspect ratio, where the changing of flow mode can happen in a non-symmetric way. When  $p/d = 1.6$ , only for consecutive experiments the flow pattern can be changed. Results of the flow visualization show many flow patterns, and the flow, after the second row becomes three-dimensional, with some vertical transversal fluctuations.

The leading feature of turbulent flow through tube banks of triangular arrangement after three, four and five rows of cylinders seems to be similar, for both aspect ratios studied. For these cases, the flow who emanates from the gaps between the cylinders presents a fast swapping, from one side to another (flip-flop). Flow visualization results show a transverse vertical component, after the second row of cylinders, which increases after the third, fourth and fifth rows, where the three-dimensional effects are more evident. Inside the tube bank a highly disordered flow is observed.

The wavelet analysis of results of hot-wire measurement together with flow visualization technique has shown to be helpful for the identification of the features of bistable flow phenomena.

## 8. REFERENCES

- Alam, M.M., Sakamoto, H. and Zhou, Y., 2005, “Determination of Flow Configurations and Fluid Forces Acting on Two Staggered Circular Cylinders of Equal Diameter in Cross-Flow”, *Journal of Fluids and Structures*, Vol. 21, pp. 363-394.
- Bendat, J. S. and Piersol, A. G., 1971, “Random Data: Analysis and Measurement Procedures”, Wiley-Interscience.
- Blevins, R. D., 1990, “Flow-Induced Vibration”, 2nd edition, Van Nostrand Reinhold, New York.
- Endres, L. A. M., Silva, C., and Möller, S. V., 1995, “Experimental Study of Static and Dynamic Fluid Flow Loads in Tube Banks”, *Transactions of the 13<sup>th</sup> International Conference on Structural Mechanics in Reactor Technology (SMiRT 13)*, Porto Alegre, Brazil.
- Endres, L. A. M. and Möller, S. V., 2001, “Looking For Correct Dimensionless Parameters For Tube-Bank Flow Analysis”, *Journal of Fluid and Structures*, Vol. 15, pp. 737-750.
- Indrusiak, M. L. S., 2004, “Characterization of Transient Turbulent Flows Using Wavelet Transform” (in Portuguese) D. Eng. Dissertation, PROMEC, Federal University of Rio Grande do Sul, Porto Alegre, Brazil, 120 p.
- Indrusiak, M. L. S., Olinto, C. R., Goulart, J. V. and Möller, S. V., 2005, “Wavelet Time-Frequency Analysis of Accelerating and Decelerating Flows in a Tube Bank”, *Nuclear and Engineering Design*, Vol. 235, pp. 1875-1887.
- Kim, H. J. and Durbin, P. A., 1988, “Investigation of the Flow between a Pair of Circular Cylinders in the Flopping Regime”, *Journal of Fluid Mechanics*, Vol. 196, pp. 431-448.
- Olinto, C. R., 2005, “Experimental Study of Turbulent Flow Characteristics in the First Bank Tubes Rows”, (in Portuguese) D. Eng. Dissertation, PROMEC, Federal University of Rio Grande do Sul, Porto Alegre, Brazil, 120 p.
- Olinto, C. R., Indrusiak, M. L. S., Möller, S. V., 2006, “Experimental Study of the Bistable Flow in Tube Arrays”, *Journal of the Brazilian Society of Mechanical Sciences and Engineering (ABCM)*, Vol. XXVIII, pp. 233-241.
- Païdoussis, M. P., 1982, “A Review of Flow-Induced Vibrations in Reactors and Reactors Components”, *Nuclear Engineering and Design*, Vol. 74, pp. 31-60.
- Sumner, D., Wong, S. S. T., Price, S. J. and Païdoussis, 1999, “Fluid Behavior of Side-By-Side Circular Cylinders in Steady Cross-Flow”, *Journal of Fluids and Structures*, Vol. 13, pp. 309-338.
- Williamson, C. H. K., 1985, “Evolution of a Single Wake Behind a Pair of Bluff Bodies”, *Journal of Fluid Mechanics*, Vol. 159, pp. 1-18.
- Zdravkovich, M. M., 1997, “Flow around circular cylinders - Volume 2: Applications”, Oxford Universit Press Inc., New York, United States, 589 p.
- Zdravkovich, M. M. and Stonebanks, K. L., 2000, “Intrinsically Non-Uniform and Metastable Flow in a Behind Tube Arrays”, *Journal of Fluids and Structures*, Vol. 4, pp. 305-319.
- Ziada, S., 2006, “Vorticity Shedding and Acoustic Resonance in Tube Bundles”, *Journal of the Brazilian Society of Mechanic Sciences and Engineering*, Vol. XXVIII, pp. 186-199.
- Žukauskas, A., 1972, “Heat Transfer from Tubes in Crossflow”, *Advances in Heat Transfer*, Vol. 8, Academic Press Inc., New York.

## 9. RESPONSIBILITY NOTICE

The authors are the only responsible for the printed material included in this paper.